

## Structural, Optical and Thermal Properties of (PEG/PAA:MnO<sub>2</sub>) Nano Composites

Areej Ahmed Mohammed <sup>1</sup>, Adnan Raad Ahmed <sup>1</sup>, Muhammad Hameed AL-TIMIMI <sup>2</sup>

1-Tikrit University, College of Education, Physics Department, Iraq.

2-University of Diyala, College of Sciences, Physics Department, Iraq.

**Abstract.** In this work, using manganese chloride and ammonia hydroxide in an aqueous solution as starting material to synthesize MnO<sub>2</sub> nanoparticles by precipitation method, The structural and optical, and thermal properties of (PEG/PAA:MnO<sub>2</sub>) Nano Composites films were investigated. The PEG/PAA polymeric blend films were doped with different ratios of MnO<sub>2</sub> nanoparticles (0, 1%, 3%, and 5%) using a casting method of  $25 \pm 1 \mu\text{m}$ . The obtained results demonstrated that the optical transmittance (%) at the wavelengths between 200-1100 nm, The optical properties of the films were affected by the MnO<sub>2</sub> ratio. The Energy gap of doped films decreased from 5.32 eV to 4.92 eV by increasing the doping (MnO<sub>2</sub>) ratios. The thermal conductivity coefficient (K) increases when adding (MnO<sub>2</sub>) nanoparticles to the polymeric mixture (PAA/PEG).

Keywords: PAA, PEG, MnO<sub>2</sub>, Structural, Optical, Thermal Properties.

### 1. Introduction

Recently, researchers and manufacturers become interested in polymers and polymerization because of their extensive applications in petrochemical and other industries. Practical techniques used with polymers may be different from composites with low molecular weights [1]. Hundreds of centuries ago, man used natural polymers including cotton, animal skins, wool, silk, etc. in the manufacture of clothes and housing, as well as food such as vegetable oils and animal fats [2]. Technological and industrial development depends heavily on the advancement of materials, as there should be alternatives due to this development. These alternatives have good specifications with low cost and lightweight; therefore, composites are produced [3].

Composites are the systems resulting from integrating two or more materials, so that each material represents a separate phase in the system, to obtain new materials with properties different from those of the raw material involved in the preparation of composite, while the undesirable properties are eliminated to be more suitable for industrial applications. The desired properties of the polymeric composite are the qualities of its basic components, which depend on matrix, reinforcement materials and interface [4-6]. Nano materials represent the distinct category of advanced materials that can be produced so that their internal granules or measures of one of their dimensions range (1-100) nm due to their

small sizes and measurements. This makes them behave contrary to the traditional large materials whose dimensions exceed (100 nm). Nano materials are building materials for the twenty-first century. They represent an important technology (nanotechnology, biotechnology and information and communication technology), which is a standard for the advancement of the civilizations and renaissance [7,8]. Polyethylene (PEG) is a small granule at room temperature, a type of thermoplastic polymers, and polyacrylic (PAA) is a colorless liquid that is soluble in water. These polymers are used as a matrix for pure and composite polymeric films. ( $\text{MnO}_2$ ) has been used through deposition method, which has several advantages, including low cost and non-toxicity. It is important to choose a method of preparation using low-cost and non-toxic materials. In addition, the properties of the prepared ( $\text{MnO}_2$ ) nanoparticles are of great importance.

The aim of this work is to synthesize  $\text{MnO}_2$  nanoparticles by precipitation method and study the structural and thermal properties of (PEG/PAA: $\text{MnO}_2$ ) Nano Composites films with different doping ratios (0, 0.01, 0.03, and 0.05) of  $\text{MnO}_2$  nanoparticles.

### 1.1 Experimental Part

( $\text{MnO}_2$ ) nanoparticles were prepared using precipitation method by adding (100 ml) of distilled water to manganese chloride by (0.5 m), then leaving it for a while until dissolved under continues stirring to obtain a homogeneous solution. Then, the ammonia hydroxide solution ( $\text{NH}_4\text{OH}$ ) with a concentration of (30%) was added gradually (drop by drop) to the primary homogeneous solution.

Pure materials consisting of (PAA/PEG) mixture were prepared using solution casting on glass Petri dish. Polymer (PAA) was mixed with polymer (PEG) by (50%) of weight mixing ratios for each by adding (0.5g) of (PAA) and (5g.0) of (PEG) to (10 ml) of distilled water at (50 °C) for (2 hours) for obtaining a homogeneous polymeric solution, After that, different weight ratios (0, 0.01, 0.03, and 0.05) from ( $\text{MnO}_2$ ) nanoparticles calcination at (800°C) were added to the mixture PAA/PEG after that using the oven for (2) days at (50 °C) in order to get rid of moisture.

## 2. Results and Discussion

### 2.1.1 Field Emission Scanning Electron Microscope (FE-SEM)

A Field Emission scanning electron microscope was used to examine the prepared samples to determine the nature of the surface and shape of ( $\text{MnO}_2$ ) nano-powder prepared using the deposition method. Figure (1) shows microscopic images of ( $\text{MnO}_2$ ) powder before and after calcination at (400,600,800°C). It can be seen that ( $\text{MnO}_2$ ) powder consists of agglomerated plates that resemble clusters, and the size of the plates increases with increasing calcination temperature[9-11] .

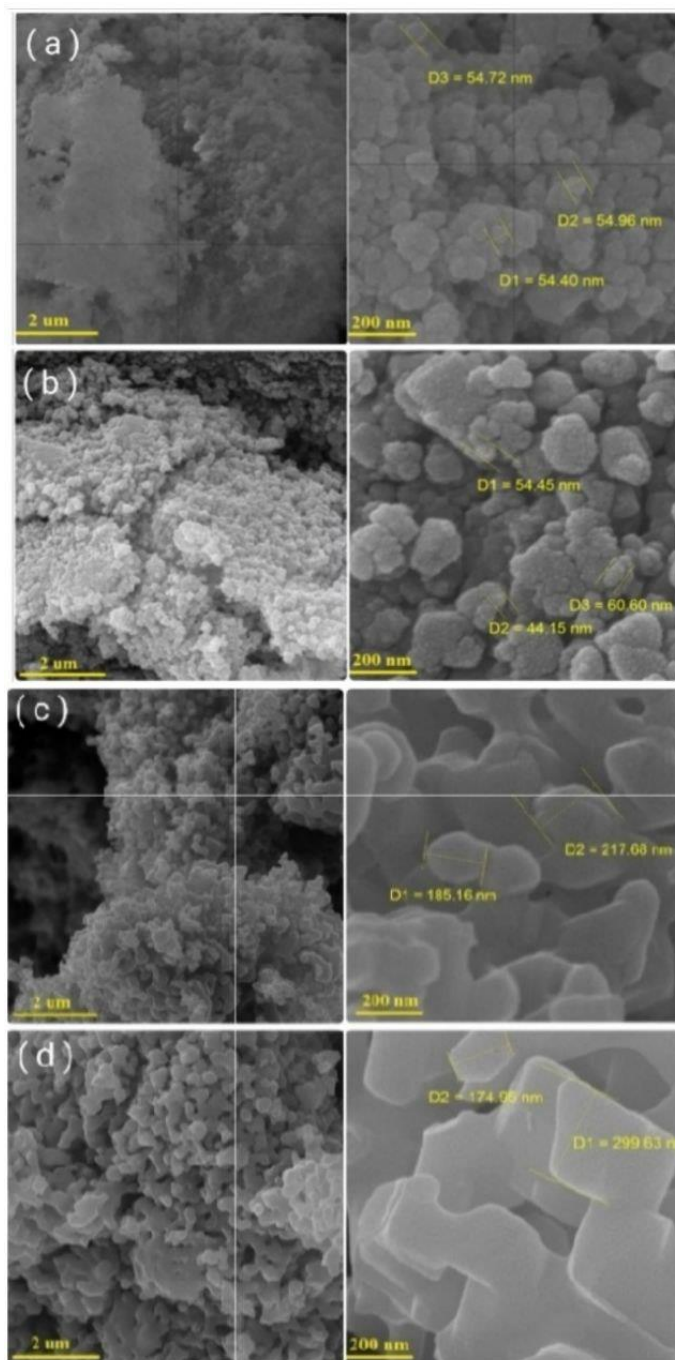


**Fig.1.** (FE-SEM) images of  $(\text{MnO}_2)$  nano-powder (a) before calcination (b) at (400 °C) (c) at (600 °C) (d) at (800 °C).

**2.1.2 Fourier-Transform Infrared Spectroscopy (FTIR)**

Infrared (FTIR) examination was conducted for all the prepared samples in order to determine the effective aggregates within the composition of the prepared samples. Figure (1) shows that multiple absorption bands were obtained. The absorption band that appears after doping with manganese oxide at ratios (1, 3 and 5) wt% centered around ( $995 \text{ cm}^{-1}$ ) and which falls within the diagnostic region (under the number The wavelength  $1000 \text{ cm}^{-1}$ ) is attributed to the expansion vibrations of manganese oxide within the structure of the

prepared nano composites [11-13]. The absorption bands detected at ( $1190\text{ cm}^{-1}$ ) and ( $1298\text{ cm}^{-1}$ ) that fall within the range ( $1180 -1300\text{ cm}^{-1}$ ) are due to the expansion vibrations of the (C-O) bond within the structure of the polymer mixture [14]. The absorption band centered around ( $1461\text{ cm}^{-1}$ ) is due to deformation vibrations of the (C-O) bond within the (PAA) polymer [15]. The absorption band centered around ( $1791\text{ cm}^{-1}$ ) indicates the stretching vibrations of the (C=O) bond within the (PEG) polymer ( $1761\text{ cm}^{-1}$ ) [16] Shifted towards a higher wave number, this change in the absorption range indicates hydrogen bonding interactions resulting from mixing the two polymers (PAA/PEG) between the (PAA) polymer framework (PAA framework) and the structure of the (PEG) polymer (PEG Backbone) [16].

Finally, the broad absorption band centered around ( $2350\text{ cm}^{-1}$ ) is due to a combination of bending vibrations of the (-OH) and expansion vibrations of the (C-H) bond [17]. We note that the interaction of nanoparticles with the polymeric chains of the polymer mixture led to a modification in the composition of the polymer mixture, where the results of the (FTIR) assay showed a difference in the intensity of the peaks and the width of the peaks of the prepared nano composites, which is due to the agglomeration and distribution of nanoparticles within the polymeric mixture (PAA/PEG). On the other hand, the results obtained showed that with the increase of the added content of manganese oxide nanoparticles, the diagnostic peaks became more clear and higher intensity.

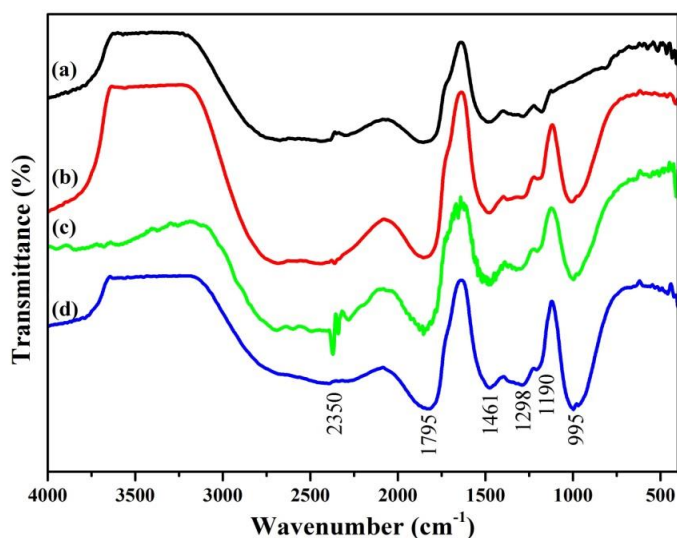
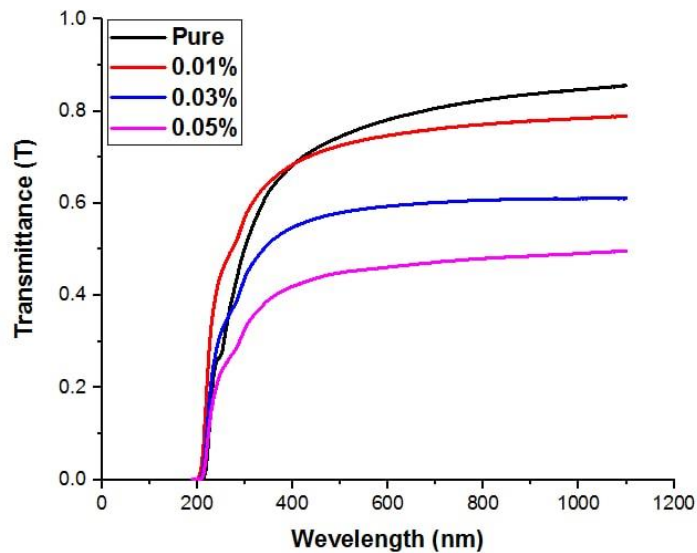


**Fig.2. FTIR spectra for (a) polymer mixture (PAA/PEG), pure and reinforced with different rates (b) 1 wt% (c) 3 wt%, and (d) 5 wt% of (MnO<sub>2</sub>) nanoparticles at (800 °C).**

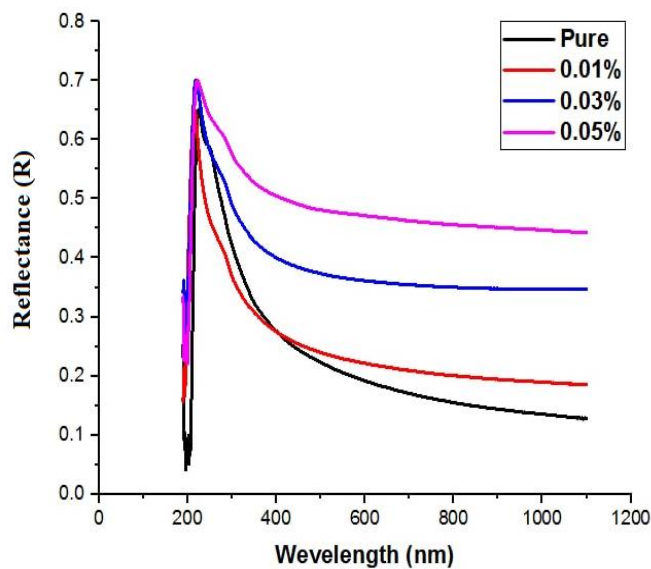
## 2.2 Optical Properties

Figure (3) and (4) shows the spectrum of transmittance (T) and reflectivity (R) of pure (PAA/PEG) films supported by different ratios of calcined manganese dioxide (MnO<sub>2</sub>) particles at (800 °C), through the obtained results. The addition of manganese dioxide (MnO<sub>2</sub>) particles leads to a decrease in the transmittance ratio (PAA/PEG) and this decrease increases for the (prepared) film, and increases when adding manganese

dioxide ( $MnO_2$ ) particles, as well as when the particle content increases, the wavelength of the incident light increases, and the ratio of The reflection, due to the emission of manganese dioxide ( $MnO_2$ ) molecules across the prepared membrane (PAA/PEG), absorbs part of the light falling on the films and fades from the other part. [18]

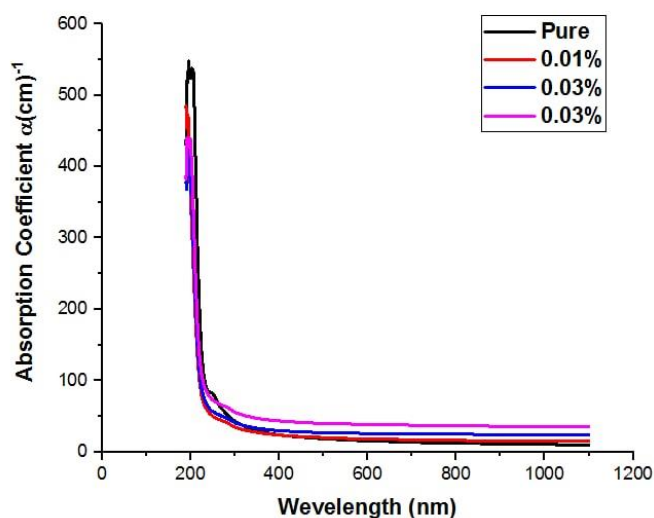


**Fig.3. Transmittance of (PAA/PEG: $MnO_2$ ) Composites.**



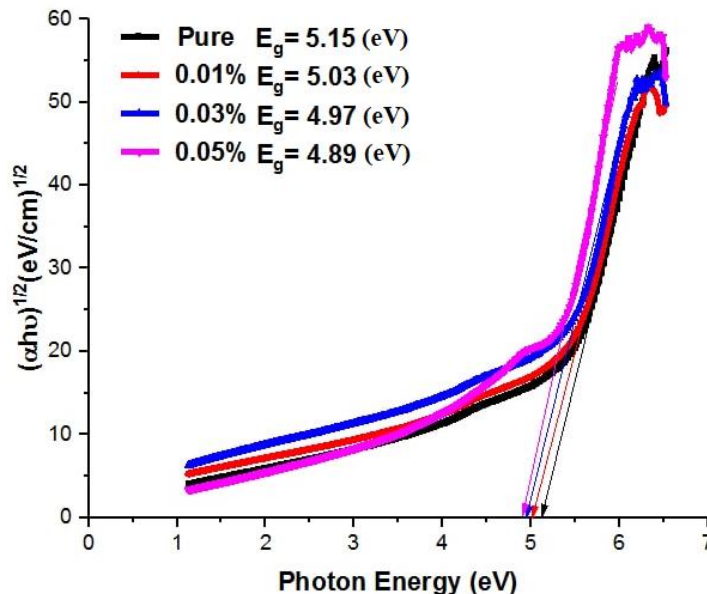
**Fig.4. Reflectance of (PAA/PEG: $MnO_2$ ) Composites.**

Fig. (5) shows the absorption coefficient of all the prepared films increases at high energies and decreases at low energy of the photon, meaning that the transmission of the electron has a high potential, that is, the energy of the incident photon is sufficient to transfer the electron from the valence bundle to the conduction bundle. The absorption coefficient helps to identify the nature of the electron. Increasing the proportion of ( $\text{MnO}_2$ ) nanoparticles leads to an increase in the absorption coefficient, and this leads to an increase in the number of charge carriers and an increase in the absorbance and absorption coefficient of films Composites [19-21].



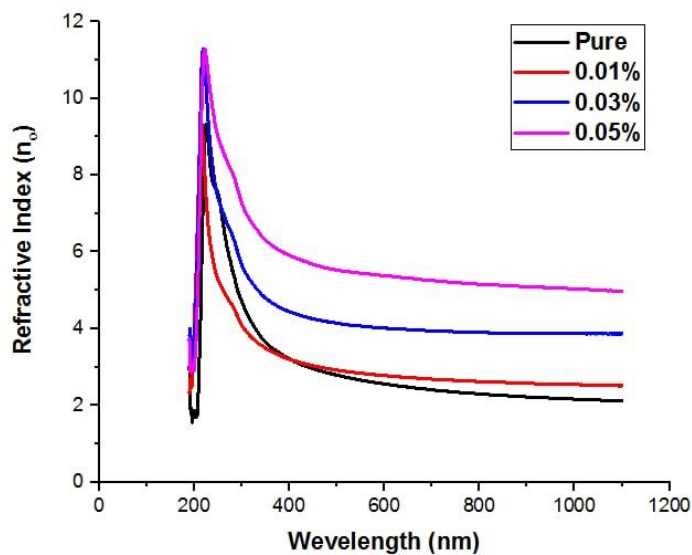
**Figure 5. Absorption Coefficient of (PAA/PEG: $\text{MnO}_2$ ) Composites.**

Fig. (6) shows that the energy gap value of the pure (PAA/PEG) film was recorded (5.15 eV), while the energy gap values of the reinforced films decreased with the increase in the content of calcined manganese oxide ( $\text{MnO}_2$ ) nanoparticles at (800 °C) to become (5.03, 4.97, 4.89) eV for particle reinforcement ratios (1%, 3%, 5%), respectively, and this decrease is the result of the content of manganese oxide ( $\text{MnO}_2$ ) nanoparticles being responsible for the formation of some defects in the films. These defects are in the optical energy gap in localized states and lead to a decrease in the optical energy gap values when the content of nanoparticles in the polymeric substrate increases [22].



**Figure 6. Energy Gap of (PAA/PEG:MnO<sub>2</sub>) Composites.**

Refractive index ( $n_o$ ) and Extinction Coefficient ( $k_o$ ), as shown in Figure (7) and (8). It shows the increase in the refractive index and inertia of pure (PAA / PEG) films when adding (MnO<sub>2</sub>) nanoparticles, and that these elements are proportional to the refractive index and with the inertia with increasing the refractive index leads to an increase in the density of stacking. For prepared films due to the increased content of nanoparticles [23].



**Figure (7): Refractive Index for (PAA/PEG:MnO<sub>2</sub>) Composites.**

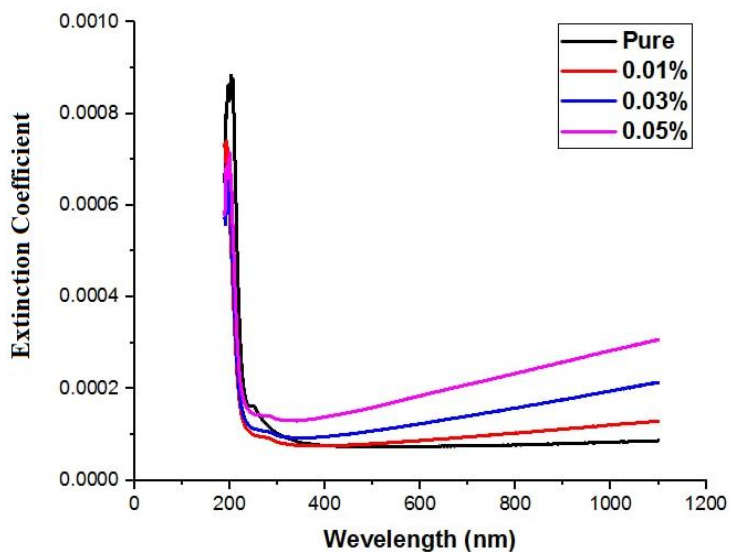


**Figure (8): Extinction Coefficient for (PAA/PEG:MnO<sub>2</sub>) Composites**

Figure (9),(10) shows the real part ( $\epsilon_r$ ) and imaginary part ( $\epsilon_i$ ) of the dielectric constant as a function of the photon energy for (PAA/PEG:MnO<sub>2</sub>) films. The results showed that adding (MnO<sub>2</sub>) nanoparticles to the polymeric mixture film (PAA/PEG) leads to an increase in the values of both the real part and the imaginary part of the dielectric constant and this increase is directly proportional to the content of the added particles, and through Figure (10) this behavior shows that increasing the content of nanoparticles leads to an increase in the electric polarization inside the reinforced films. The increase in the dielectric constant of the polymeric mixture (PAA/PEG) represents a partial increase in the charges inside the polymers. We also note the change of the real part and the imaginary part of the reinforced (PAA/PEG) films, and the real part of the dielectric constant depends on the refractive index, and the imaginary part of the dielectric constant depends on the damping coefficient. [24]

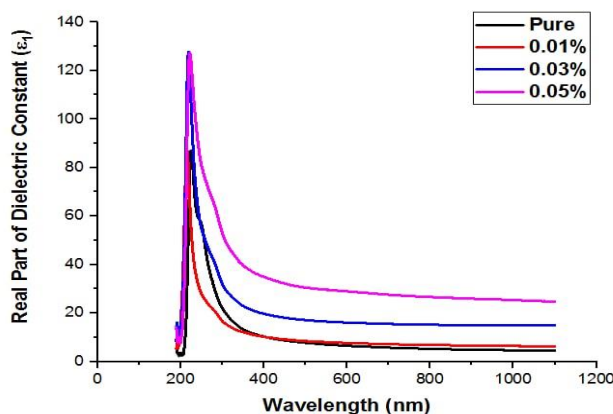


**Fig. (3-1) : Real Part of the Dielectric Constant for (PAA/PEG:MnO<sub>2</sub>) Composites.**

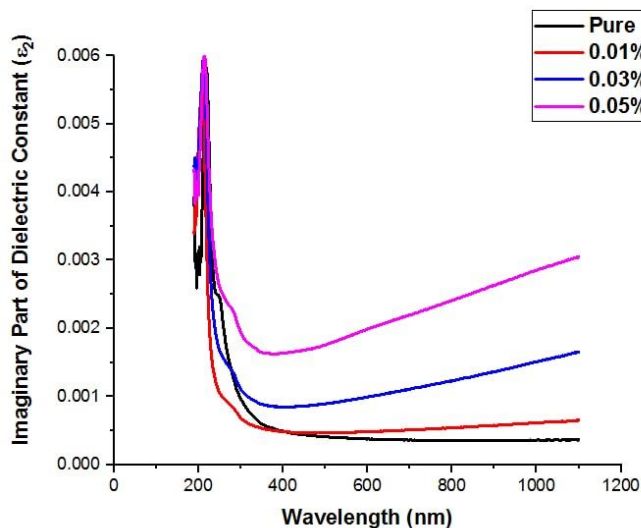


**Fig. ():**Imaginary Part of the Dielectric Constant for (PAA/PEG:MnO<sub>2</sub>) Composites.

### 3.3 Thermal Conductivity

The conduction coefficient (K) values were calculated for the models prepared through (the Li disk). Figure (5) shows the thermal conductivity (K) coefficients of the as-prepared polymeric films (PAA/PEG) before and after reinforcement with different ratios (1%, 3%, 5%) with calcined manganese oxide (MnO<sub>2</sub>) nanoparticles at (800 °C). the obtained results showed that the thermal conductivity coefficient (K) increases when manganese oxide (MnO<sub>2</sub>) particles are added to a poly (PAA/PEG) mixture, Also by increasing the weight ratio of the manganese oxide particles, the thermal conductivity coefficient increases widely. The model (PAA/PEG): 15% (MnO<sub>2</sub>) at (800 °C) recorded the highest value of the thermal conductivity coefficient, which shows in Table (1-1) that the reason for the increase in the coefficient values Thermal conductivity (K) is that the addition of particles to polymeric materials leads to an improvement in the thermal conductivity properties due to filling the polymer with nanoparticles, Additive nanoparticles (MnO<sub>2</sub>) are materials with high thermal conductivity compared to polymeric mixture (PAA/PEG) due to the difference in structural composition between them [25-27].

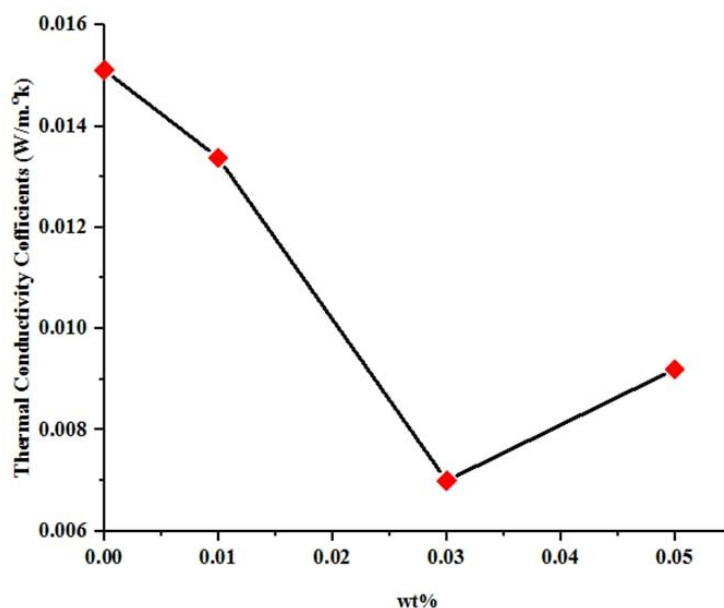


**Fig.5. Thermal Conductivity Coefficient for (PAA/PEG:MnO<sub>2</sub>) Composites.**

The proportion of the uniform conductive medium within the random polymer mixture, the decrease in the possibility of phonons scattering within complex structures, and the increase in the thermal conductivity coefficient of the prepared films increases with the increase in the proportion of manganese oxide particles [28]. The polymer mixture (PAA/PEG) recorded the lowest value for the coefficient of thermal conductivity. The addition of the polymer (PEG) to the polymer (PAA) increases the random medium within the polymer mixture and leads to a high probability of scattering the phonons responsible for the thermal energy transfer process in the insulating materials, due to the presence of a fracture in the structure and the transition from one structure to another leads to the difficulty of transferring thermal energy. Between the two different random phases (PEG) and (PAA) in the form of elastic waves due to the presence of a spacer in the structure and this part of the wave energy will check and then decrease the thermal conductivity coefficient of the polymeric mixture [29].

## Conclusion

The FE-SEM results show that particles size increases with the increase in calcination temperature. Diagnostic peaks become more visible and more severe with the increase in the content of manganese dioxide (MnO<sub>2</sub>) nanoparticles. The absorption band that appears after doping with manganese oxide at ratios (1, 3 and 5) wt% centered around (995 cm<sup>-1</sup>) and which falls within the diagnostic region (under the number The wavelength (1000 cm<sup>-1</sup>) is attributed to the expansion vibrations of manganese oxide within the structure of the

prepared nano composites. The addition and increase of (MnO<sub>2</sub>) content led to a decrease in transmittance of (PAA/PEG) film prepared, while its reflectance rate increased. The absorption coefficient for all prepared films increased at high energies and decreased with the decrease in photon energy. The band gap values of reinforced films decreased with the increase in (MnO<sub>2</sub>) content at (800 °C). The values of refractive index and extinction coefficient of pure (PAA/PEG) films increased when adding (MnO<sub>2</sub>) content at (800 °C). The addition of (MnO<sub>2</sub>) nanoparticles to the polymeric mixture (PAA/PEG) film increased the values of the real and imaginary parts for dielectric constant relative static permittivity. Finally, thermal conductivity coefficient (K) increased when adding (MnO<sub>2</sub>) nanoparticles to the polymeric mixture (PAA/PEG).

## References

- [1] Rasheed, H. S. (2019). The Effect of Adding PAA on the Physical Properties of PEG. *Annals of the University of Craiova: Physics AUC*, 29, 36-44.
- [2] Myung, D., Waters, D., Wiseman, M., Duhamel, P. E., Noolandi, J., Ta, C. N., & Frank, C. W. (2008). Progress in the development of interpenetrating polymer network hydrogels. *Polymers for advanced technologies*, 19(6), 647-657.
- [3] Nguyen, M. K., & Lee, D. S. (2010). Bioadhesive PAA-PEG-PAA triblock copolymer hydrogels for drug delivery in oral cavity. *Macromolecular Research*, 18(3), 284-288.
- [4] Liu, Z., Tang, B., & Zhang, S. (2020). Novel network structural PEG/PAA/SiO<sub>2</sub> composite phase change materials with strong shape stability for storing thermal energy. *Solar Energy Materials and Solar Cells*, 216, 110678.
- [5] Sill, K. N., Sullivan, B., Carie, A., & Semple, J. E. (2017). Synthesis and Characterization of Micelle-Forming PEG-Poly (Amino Acid) copolymers with iron-hydroxamate cross-linkable blocks for encapsulation and release of hydrophobic drugs. *Biomacromolecules*, 18(6), 1874-1884.
- [6] Cui, M., & Lee, P. S. (2016). Solid polymer electrolyte with high ionic conductivity via layer-by-layer deposition. *Chemistry of Materials*, 28(9), 2934-2940.
- [7] Shivashankar, M., & Mandal, B. K. (2012). A review on interpenetrating polymer network. *Int. J. Pharm. Pharm. Sci*, 4(5), 1-7.
- [8] Al-Zanganawee, J., Al-Timimi, M., Pantazi, A., Brincoveanu, O., Moise, C., Mesterca, R., ... & Enachescu, M. (2016). Morphological and optical properties of functionalized SWCNTs: P3OT nanocomposite thin films, prepared by spincoating. *Journal of Ovonic Research*, 12(4), 201-207.

- [9] Haoran, Y., Lifang, D., Tao, L., & Yong, C. (2014). Hydrothermal synthesis of nanostructured manganese oxide as cathodic catalyst in a microbial fuel cell fed with leachate. *The Scientific World Journal*, 2014.
- [10] Akbari, S., Mehdi, M., & Foroughi, M. (2018). Solvent-free synthesis and characterization of MnO<sub>2</sub> nanostructures and investigation of optical properties. *J Nanomed Nanotechnol*, 9(498), 2.
- [11] Shaker, K. S., & AbdAlsalm, A. H. (2018). Synthesis and characterization nano structure of MnO<sub>2</sub> via chemical method. *Engineering and Technology Journal*, 36(9 Part A).
- [12] Sahai, A., & Goswami, N. (2014). Structural and vibrational properties of ZnO nanoparticles synthesized by the chemical precipitation method. *Physica E: Low-dimensional Systems and Nanostructures*, 58, 130-137.
- [13] Dutta, S., & Ganguly, B. N. (2012). Characterization of ZnO nanoparticles grown in presence of Folic acid template. *Journal of nanobiotechnology*, 10(1), 1-10.
- [14] Abdullah, M. Z., Al-Timimi, M. H., Albanda, W. H., Dumitru, M., Balan, A. E., Ceaus, C., ... & Stamatina, I. (2019). STRUCTURAL AND ELECTROCHEMICAL PROPERTIES OF P<sub>3</sub>-Na<sub>0.67</sub>Mn<sub>0.3</sub>Co<sub>0.7</sub>O<sub>2</sub> NANOSTRUCTURES PREPARED BY CITRIC-UREA SELFCOMBUSTION ROUTE AS CATHODE FOR SODIUM ION BATTERY. *DIGEST JOURNAL OF NANOMATERIALS AND BIOSTRUCTURES*, 14(4), 1179-1193.
- [15] Moussa, S., Namouchi, F., & Guermazi, H. (2015). Elaboration, structural and optical investigations of ZnO/epoxy nanocomposites. *The European Physical Journal Plus*, 130(7), 1-9.
- [16] Yuan, S., Tang, Q., Hu, B., Ma, C., Duan, J., & He, B. (2014). Efficient quasi-solid-state dyesensitized solar cells from graphene incorporated conducting gel electrolytes. *Journal of Materials Chemistry A*, 2(8), 2814-2821.
- [17] Li, R., Wu, Y., Bai, Z., Guo, J., & Chen, X. (2020). Effect of molecular weight of polyethylene glycol on crystallization behaviors, thermal properties and tensile performance of polylactic acid stereocomplexes. *RSC Advances*, 10(69), 42120-42127.
- [18] Nam, J., Kim, E., KK, R., Kim, Y., & Kim, T. H. (2020). A conductive self healing polymeric binder using hydrogen bonding for Si anodes in lithium ion batteries. *Scientific reports*, 10(1), 1-12.
- [19] Hashim, A., & Habeeb, M. A. (2019). Synthesis and characterization of polymer blend-CoFe<sub>2</sub>O<sub>4</sub> nanoparticles as a humidity sensors for different temperatures. *Transactions on Electrical and Electronic Materials*, 20(2), 107-112.

- [20] Agool, I. R., Kadhim, K. J., & Hashim, A. (2017). Fabrication of new nanocomposites (PVA-PEG-PVP) blend-zirconium oxide nanoparticles) for humidity sensors. *International Journal of Plastics Technology*, 21(2), 397-403.
- [21] Sangawar, V., & Golchha, M. (2013). Evolution of the optical properties of polystyrene thin films filled with zinc oxide nanoparticles. *International Journal of Scientific & Engineering Research*, 4(6), 2700-2705.
- [22] Hashim, A., & Hadi, Q. (2018). Structural, electrical and optical properties of (biopolymer blend/titanium carbide) nanocomposites for low cost humidity sensors. *Journal of Materials Science: Materials in Electronics*, 29(13), 11598-11604.
- [23] Wang, B., Ma, R., Liu, G., Liu, X., Gao, Y., Shen, J., ... & Shi, L. (2010). Effect of Coordination on the Glucose-Responsiveness of PEG-b-(PAA-co-PAAPBA) Micelles. *Macromolecular rapid communications*, 31(18), 1628-1634.
- [24] Hashim, A., Agool, I. R., & Kadhim, K. J. (2018). Novel of (polymer blend-Fe<sub>3</sub>O<sub>4</sub>) magnetic nanocomposites: preparation and characterization for thermal energy storage and release, gamma ray shielding, antibacterial activity and humidity sensors applications. *Journal of Materials Science: Materials in Electronics*, 29(12), 10369-10394.
- [25] Lee, S.H., & Ohkita, T. (2003). Mechanical and thermal flow properties of wood flour-biodegradable polymer composites. *Journal of applied polymer science*, 90(7), 1900-1905.
- [26] Salman, S. A., Abdu-allah, M. H., & Bakr, N. A. (2014). Optical characterization of red methyl doped poly (vinyl alcohol) films. *International Journal of Engineering and Technical Research*, 2(4), 126-128.
- [27] Hashim, A., & Hadi, Q. (2018). Synthesis of novel (polymer blend/ceramics) nanocomposites: structural, optical and electrical properties for humidity sensors. *Journal of Inorganic and Organometallic Polymers and Materials*, 28(4), 1394-1401.
- [28] W. Callister, (1994), "Material Science & Engineering, An Introduction", Third Edition, John Wiley & Sons Inc.
- [29] Childs, G. E., Ericks, L. J., & Powell, R. L. (1973). Thermal conductivity of solids at room temperature and below: A review and compilation of the literature.